ALPN-101 (Acazicolcept) a Dual ICOS/CD28 Antagonist, Demonstrates Efficacy in Systemic Sclerosis Preclinical Mouse Models

Cindy Orvain
INSERM U1016: Institut Cochin
Anne Cauvet
INSERM U1016: Institut Cochin
Alexis Prudent
INSERM U1016: Institut Cochin
Christophe Guignabert
INSERM U999: Hypertension Pulmonaire Physiopathologie et Nouvelles Therapies
Raphaël Thuillet
INSERM U999: Hypertension Pulmonaire Physiopathologie et Nouvelles Therapies
Mina Ottaviani
INSERM U999: Hypertension Pulmonaire Physiopathologie et Nouvelles Therapies
Ly Tu
INSERM U999: Hypertension Pulmonaire Physiopathologie et Nouvelles Therapies
Fanny Duhalde
INSERM U1016: Institut Cochin
Carole Nicco
INSERM U1016: Institut Cochin
Frédéric Batteux
INSERM U1016: Institut Cochin
Jérôme Avouac
INSERM U1016: Institut Cochin
NinXin Wang
Alpine Immune Sciences
Michelle A. Seaberg
Alpine Immune Sciences
Stacey R. Dillon
Alpine Immune Sciences
Yannick Allanore (yannick.allanore@me.com)
Universite Paris Descartes

Research article

Keywords: Systemic sclerosis, Dermal fibrosis, Pulmonary fibrosis, Pulmonary hypertension, Co-stimulation blockade, ICOS, CD28

Posted Date: September 28th, 2021

DOI: https://doi.org/10.21203/rs.3.rs-915978/v1

Version of Record: A version of this preprint was published at Arthritis Research & Therapy on January 5th, 2022. See the published version at https://doi.org/10.1186/s13075-021-02709-2.

Abstract

Background

Uncontrolled immune response with T cell activation has a key role in the pathogenesis of systemic sclerosis (SSc), a disorder that is characterised by generalized fibrosis affecting particularly the lungs and skin. Co-stimulatory molecules are key players during immune activation, and recent evidence supports a role of CD28 and ICOS in the development of fibrosis. We herein investigated the efficacy of ALPN-101 (acazicolcept), a dual ICOS/CD28 antagonist, in two complementary SSc-related mouse models recapitulating skin fibrosis, interstitial lung disease, and pulmonary hypertension.

Methods

Expression of circulating soluble ICOS and skin-expressed ICOS was investigated in SSc patients. Thereafter, ALPN-101 was evaluated in the hypochlorous acid (HOCL)-induced dermal fibrosis mouse model and in the Fra-2 transgenic (Tg) mouse model. In each model, mice received 400 µg of ALPN-101 or a molar-matched dose of an Fc control protein twice a week for six weeks. After six weeks, skin and lung were evaluated.

Results

ICOS was significantly increased in the sera from SSc patients and in SSc skin biopsies as compared to samples from healthy controls. Similar body weight changes were observed between Fc Control and ALPN-101 groups in both HOCL and Fra-2 Tg mice suggesting a good tolerance of ALPN-101 treatment. In mice challenged with HOCL, ALPN-101 induced a significant decrease in dermal thickness, collagen content, myofibroblast number and inflammatory infiltrates characterized by B cells, T cells, neutrophils, and macrophages. In the Fra-2 Tg mouse model, ALPN-101 treatment reduced lung collagen content, fibrillar collagen, histological fibrosis score, and right ventricular systolic pressure (RVSP). A reduction in frequency of CD4+ and T effector memory cells and an increase in the percentage of CD4+ T naïve cells in spleen and lung of ALPN-101-treated Fra-2 Tg mice was observed as compared to Fc control-treated Fra-2 Tg mice. Moreover, ALPN-101 reduced CD69 and PD-1 expression on CD4+ T cells from the spleen and the lung. Target engagement by ALPN-101 was demonstrated by blockade of CD28 and ICOS detection by flow cytometry in treated mice.

Conclusions

Our results confirm the importance of co-stimulatory molecules in inflammatory-driven fibrosis. Our data highlight a key role of ICOS and CD28 in SSc. Using complementary models, we demonstrated that dual ICOS/CD28 blockade by ALPN-101 decreased dermal and pulmonary fibrosis and alleviated pulmonary hypertension. These results pave the way for subsequent research on ICOS/CD28-targeted therapies.

Introduction

Systemic sclerosis (SSc) is a rare autoimmune rheumatic disease characterized by vasculopathy and dysregulation of the immune response, and extensive fibrosis of skin and internal organs (1). This leads to increased morbidity and mortality of SSc patients mainly due to cardiovascular and pulmonary complications (2). T cells are a major component of SSc pathophysiology as indicated by their early recruitment in SSc skin (3). Several studies have shown the contribution of Th2, Th17, Th22, Tfh, and CD8 + subsets to inflammation in blood and skin of SSc patients (4). Early vascular and immune interactions are supported by the recent findings showing that endothelial cells expressing HLA-DR are targeted by cytotoxic CD4 + cells, leading to their apoptosis and likely remodelling in affected SSc tissue (5). T cell activation, proliferation, and differentiation are based on an appropriate interaction between T cell co-stimulation molecules and their receptors on antigen-presenting cells (APC). Co-stimulation blockade in several SSc murine models has shown to mitigate fibrosis, linking T cell activation and fibrosis/remodelling development (6).

CD28 and inducible T cell costimulator (ICOS) are closely related T cell costimulatory molecules within the immunoglobulin superfamily that bind, respectively, the ligands CD80 and CD86, and ICOS ligand (ICOSL), and play partially overlapping roles in immunity (7). Signalling through CD28 and ICOS leads to T cell cytoskeletal remodelling, production of cytokines, enhanced survival, and differentiation (8, 9). CD28 and ICOS also cooperate in lung mucosa to induce differentiation of Th2 effector cells (10). The concept of interfering with T cell costimulation to treat autoimmune diseases has been clinically validated with abatacept (CTLA-4-Ig), an approved CD28 pathway inhibitor for rheumatoid arthritis, juvenile idiopathic arthritis, and psoriatic arthritis.

The CD28 pathway inhibitor abatacept was evaluated in a phase II trial (ASSET) in early diffuse cutaneous SSc (dcSSc). Although abatacept was well-tolerated in the ASSET trial, patients treated with abatacept did not experience significantly greater improvements of the modified Rodnan Skin Score (mRSS) than those administered placebo, though some improvements in secondary outcome measures were observed in the abatacept arm (11). These results suggest that CD28 pathway inhibition alone is insufficient to significantly impact skin disease in dcSSc patients.

ICOS is not expressed in naïve T cells but is rapidly upregulated after activation and may represent a key pathogenic pathway unaddressed by CD28 antagonism. ICOS appears particularly important for the function of several activated and/or effector T cell subsets, including differentiated types 1, 2, and 17, as well as follicular helper T cells (TFH) (12). Indeed, activated T cells often downregulate CD28 and/or become less dependent on CD28 costimulation, and CD28-negative T cells accumulate in various inflammatory diseases, correlating with disease activity and lack of responsiveness to abatacept (13–19). In contrast, ICOS upregulation correlates with disease activity in several inflammatory diseases (20–24), and in preliminary studies, the anti-ICOSL mAb prezalumab (AMG-557) demonstrated some beneficial activity on the arthritis of systemic lupus erythematosus (NCT04058028 ; (25)), as well as on overall disease activity in Sjögren's syndrome (NCT02334306). However, at present no ICOS pathway antagonists have been approved for therapeutic use.

Preliminary data in SSc patients have demonstrated an increase of soluble ICOS in the sera of patients with diffuse cutaneous SSc (26, 27) and of ICOS + Tfh-like cells in their skin (28). Studies in SSc mouse models challenged with bleomycin indicated that ICOS-deficient mice were protected from skin and lung fibrosis (29). In a GVHD model that shares some similarities with SSc, compelling data have revealed a decrease in dermal inflammation and fibrosis after anti-ICOS antibody administration (28). Taken together, these data suggest a potential role of ICOS in inflammation-driven lung and skin fibrosis.

We hypothesized that a dual-reactive molecule that blocks both pathways, ICOS together with CD28 may be of interest in immune-related diseases; this general approach has since been shown to abrogate ongoing germinal centre reactions during an immune response (30). The blockade of CD28 and ICOS in an acute GvHD mouse model by the novel dual CD28/ICOS antagonist (ALPN-101/acazicolcept) led to improved survival in ALPN-101-treated mice compared to mice receiving a CD28-CD80/CD86 pathway antagonist (belatacept; CTLA-4-Ig) only (31). These results suggest that co-targeting ICOS and CD28 is a relevant strategy to suppress autoimmune responses (31). Therefore, we herein evaluated the therapeutic effect of ALPN-101 on immune responses and related fibrosis in two complementary mouse models mimicking the severe organ damage observed in SSc patients.

Materials And Methods

Animals

6-week-old female BALB/c mice were purchased from Janvier Laboratory (Le Genest Saint Isle, France) and experiments were conducted in a conventional facility (C75-14-05). Transgenic female Fra-2 (B6.Cg-Tg(H2-K-Fosl2,EGFP)13Wag) mice were bred in a SPF facility (C75-14-02). All mice were housed in ventilated cages with sterile food and water *ad libitum*. Animals received humane care in compliance with the guidelines implemented at our institution (INSERM and University Paris Descartes).

ALPN-101 molecule and pharmacological treatment

ALPN-101 (acazicolcept; ICOSL vIgD-Fc), provided by Alpine Immune Sciences (AIS) (Seattle, WA), is a dual human ICOS/CD28 inhibitor Fc fusion protein (31). ALPN-101 (produced at KBI Biopharma, Durham NC) and Fc control protein (produced at AIS) were diluted in PBS and injected intraperitoneally twice a week at molar-matched doses of 400 µg/mouse and 267 µg/mouse, respectively. The mouse dosing regimen was identified from prior mouse pharmacokinetic/pharmacodynamic studies as one that provided adequate exposure and disease modifying activity in multiple mouse models of autoimmunity and inflammation. However, this dosing regimen would not be used directly to predict human regimens due to species- and disease-related differences in multiple factors including target abundance, binding, and clearance.

HOCL induction of dermal fibrosis and ALPN-101 treatment

Dermal fibrosis was induced in six-week-old BALB/c mice according to the protocol described by Servettaz et al (32). A total of 400 µL hypochlorous acid (HOCl) solution was prepared extemporaneously by adding NaClO (9.6% as active chlorine) to KH_2PO_4 solution (100 mM, pH: 6.2), usually using a 1:100 ratio. The correct amount of NaClO was adjusted to obtain the desired HOCl concentration, defined by the absorbance of the mixture at 292 nm (optical density between 0.7 and 0.9). 200 µL of HOCl solution was injected intradermally into each shaved flank of the mice using a 27-gauge needle, 5 days a week for 6 weeks. Control mice were injected intradermally with 200 µL of sterilized phosphate-buffer saline (PBS) into each shaved flank. 100 µL of ALPN-101 or Fc control dosing solutions were injected intraperitoneally twice a week during the 6 weeks of HOCl-treatment. Mice were divided into the following groups : PBS (n=6), HOCL + Fc control (n=8), and HOCL + ALPN-101 (n=8). Mice were euthanized by cervical dislocation after 6 weeks of treatment (Supplementary Figure 1). This experiment has been carried out once.

Fra-2 transgenic mice and ALPN-101 treatment

Transgenic mice expressing the Fra-2 transgene under the control of ubiquitous major histocompatibility complex class I antigen H-$2K^b$ promoter develop microangiopathy, systemic inflammation, lung fibrosis, and pulmonary hypertension (33). These features follow a similar temporal sequence as observed in human SSc. In the lungs, perivascular inflammatory infiltrates and vascular remodeling appear at the 12^{th} week of age and are followed by fibrosis development at 15^{th} week of age (34). Fra-2 transgenic mice display severe vascular remodeling of pulmonary arteries leading to their intimal thickening and, in the worst case, to obliteration of vessels (35). Two groups of Fra-2 transgenic female mice were treated starting at 12 weeks of age with intraperitoneal injections of ALPN-101 (n=11) or Fc control (n=8) twice a week, for a total of 6 weeks. Mice were euthanized by exsanguination after right ventricular systolic pressure (RVSP) measurement at 18 weeks of age (Supplementary Figure 2). This experiment has been carried out twice.

ALPN-101 serum measurement

The concentration of ALPN-101 was measured in serum samples collected 24 hours after the 8^{th} or 13^{th} dose in the HOCL model, or after the 10^{th} and 13^{th} dose in the Fra-2 Tg model, using an ELISA method developed at Alpine Immune Sciences. ALPN-101 was captured by Fc-specific donkey anti-human IgG antibody (Jackson ImmunoResearch), immobilized onto a 96-well microtiter plate and detected with $F(ab')_2$ fragment, Fc-specific donkey anti-huIgG:HRP (Jackson ImmunoResearch). A calibration curve was generated for each assay plate using SoftMax Pro data acquisition and analysis software (version 7.1, Molecular Devices).

Clinical follow-up of Fra-2 mice

Fra-2 transgenic mice developed a disease phenotype requiring their clinical follow-up. Monitoring included weighing the mice once a week for the duration of the experiment. All the mice were scored

individually using body weight change and observation of their physical appearance and behavior. Mice received a clinical score of 0 to 3, with 0 = normal ; 1 = weight loss <10%, lack of grooming and behavior minor modifications ; 2 = weight loss between 10-15%, alopecia and skin lesions, reduced mobility, Raynaud's syndrome ; 3 = weight loss > 20%, ruffled fur, hunched posture, lethargy. If mice reached a clinical score of 3 before the end of the experiment, they were euthanized to respect the 3R rule.

Skin thickness measurement of HOCL-treated mice

Skin thickness (expressed in millimeters) was assessed using a caliper to measure the dermal thickness of the shaved backs of the mice. The measurement was performed once a week until the end of the experiment.

Collagen measurement

Collagen content was measured in a 3-mm punch from the back skin of HOCL-treated mice or from lung biopsies (right lobes) of Fra-2 mice using Sircol® soluble collagen assay (Biocolor, UK) according to the manufacturer's instructions. Collagen content was determined from the slope of the standard curve calculated using known collagen concentrations.

Immunohistochemistry and immunofluorescence

Paraffin-embedded sections of dorsal skin were obtained from (1) PBS/, HOCL/Fc control- and HOCL/ALPN-101-treated mice, and (2) healthy or lesional skin biopsies obtained from healthy human controls or SSc patients. After antigen retrieval, blocking and tissue permeabilization with PBS + 0.25% Triton X-100, mouse skin sections were incubated with the following primary antibodies diluted in PBS+0.5% BSA overnight at 4°C : rat anti-CD3 (Abcam, clone RM0027-3B19, dilution : 1/50), rabbit anti-CD68 (Abcam, Polyclonal, dilution : 1/250), rat anti-CD20 (Abcam, clone GOT214A, dilution : 1/100), rat anti-Ly6G (BD Biosciences, Clone 1A8, dilution : 1/500), and rabbit anti-alpha-SMA (Abcam, Clone E184, dilution : 1/250). Then, slides were incubated with the following secondary antibodies diluted in PBS + 1% BSA for one hour at RT : goat anti-rabbit (Pierce, dilution : 1/200) and goat anti-rat (Invitrogen, dilution : 1/500 for Ly6G and CD20 ; 1/150 for CD3). Visualization was performed with Dako Liquid DAB+Substrate Chromogen System (Agilent Technologies), slides were counterstained with hematoxylin (ThermoFisher) and mounted using aqueous mounting medium (Merck Millipore). For human skin sections, the following primary antibodies diluted in PBS+0.5% BSA were incubated overnight at 4°C : anti-ICOS (Abcam goat polyclonal, dilution : 1/130) and anti-CD3 (Abcam Clone CD3-12, dilution : 1/250). Then, slides were incubated with the following secondary antibodies diluted in PBS+1% BSA for one hour at RT : anti-goat AF594 (ThermoFisher, dilution 1/200) and anti-rat AF488 (Thermofisher, dilution 1/200). Slides were mounted using Vectashield® mounting medium with DAPI (Vector Laboratories, UK). Analysis of the immunostaining was performed using the Lamina Multilabel Slide Scanner (Perkin Elmer, USA). Slide staining analysis was performed with CaseViewer software (version 2.4).

Histopathologic assessment of dermal fibrosis in HOCL-treated mice and fibrosing alveolitis in the Fra-2 model

Fixed 6-mm skin punch biopsies from HOCL-treated mice or left lung from Fra-2 mice were embedded in paraffin. A 4-µm thick tissue section was stained with hematoxylin, eosin, and saffron. Slides were scanned with the Lamina Multilabel Slide Scanner. For HOCL skin sections, dermal thickness was evaluated at 100-fold magnification by measuring the distance between the epidermal-dermal junction and the dermal-subcutaneous fat junction at five sites on skin sections by two independent blinded examiners with the CaseViewer software (version 2.4). The mean of the 10 values obtained by the two examiners was calculated for each skin section. For Fra-2 Tg lung sections, the severity of fibrosing alveolitis was semi-quantitatively assessed by examining the entire slide, by two examiners blinded to the treatment. The grading criteria were as follows: 0 = normal lung ; 1 = Minimal fibrous thickening of alveolar or bronchioalveolar walls ; 2-3 = moderate thickening of walls without obvious damage to lung architecture ; 4-5 = Increased fibrosis with definite damage to lung structure and formation of fibrous bands or small fibrous masses ; 6-7 = Severe distortion of structure and large fibrous areas and 8 = Total fibrous obliteration (36).

Nonlinear microscopy and second harmony generation (SHG) processing

A 2-photon Leica SP8 DIVE FLIM (Leica Microsystems GmbH, Wetzlar, Germany) was used for lung and skin tissue imaging. Two lasers at 1040 and 880 nm wavelength were used to generate second harmonic (SHG) and two-photon-excited fluorescence (TPEF) signals, collected by a Leica Microsystems HCX IRAPO 25×/0.95 W objective and two external detectors. Microscopy was performed on 16 µm-thick blank blades of sliced lungs or skin. Five samples of each slice were taken. The SHG score was established by comparing the area occupied by the collagen relative to the sample surface. Image processing and analysis (thresholding and SHG scoring) were performed using ImageJ homemade routine as previously described (37).

Right ventricular systolic pressure (RVSP) measurement in Fra-2 mice

RVSP was assessed in unventilated mice under isoflurane anesthesia (1.5-2.5%, 2L O_2/min) using a closed chest technique by introducing a catheter (1.4-F catheter; Millar Instruments Inc., Houston, TX) into the jugular vein and directing it to the right ventricle. After RVSP measurement, blood was collected by direct cardiac puncture leading to mouse sacrifice. The heart and lungs were removed and flushed with 5 mL of buffered saline at 37°C. The left lung was fixed in paraformaldehyde 4%. For 10 Fra-2 Tg mice (4 Fc control- and 6 ALPN-101-treated), one lobe of the right lung was collected to perform FACS analysis and other lobes were immediately snap-frozen in liquid nitrogen and kept at -80°C.

Spleen and lung cell isolation for flow cytometry staining

Flow cytometry staining was performed on 4 spleen/lung Fc control-treated mice and on 6 spleen/lung ALPN-101-treated mice. Spleens were collected and crushed on a 70 µm cell strainer. Red cells were

removed with ACK Lysing Buffer (Thermofisher). $1x10^6$ cells were collected for flow cytometry staining. One lung lobe was cut in small pieces and incubated in PBS 10% FBS + Collagenase II (1mg/mL, StemCell Technologies) and DNase I (0.1mg/mL, StemCell Technologies) for 1 hour at 37°C. After mechanical dissociation with vortexing, cell suspensions were passed through a 70 µm cell strainer. Red blood cells were removed with ACK Lysing Buffer (ThermoFisher). A Percoll (Sigma) density gradient was generated by resuspending cells in a 40% Percoll solution and adding an 80% Percoll solution below the 40% solution. The cell ring was collected, and the total lung cell suspension was used for flow cytometry staining.

Spleen and lung cells were incubated with Zombie Dye UV (Biolegend) for 15 minutes at room temperature. Fc receptors were blocked with the TruStain FcX™ (anti-mouse CD16/32) Antibody (Clone 93, Biolegend) for 5 minutes on ice. Cells were first incubated with an anti-CD62L-APC/Cy7 antibody (Clone MEL-14, Biolegend) for 20 minutes on ice. Second, the following antibody mix was incubated with cells for 30 minutes on ice : anti-CD4 BV711 (Clone GK1.5), anti-CD19-AlexaFluor700 (Clone 6D5), anti-CD3-BV510 (Clone 17A2), anti-CD44-BV605 (Clone IM7), anti-CD28-BV421 (Clone 37.51), anti-CD69-BV650 (Clone H1.2F3), anti-PD-1-PE/Dazzle 594 (Clone 29F.1A12), anti-human IgG Fc-PE (clone M1310G05), anti-ICOS-APC (Clone 7E.17G9) purchased from Biolegend and anti-CD8-BUV737 (Clone 53-6.7) purchased from BD Biosciences. Stained cells were fixed in PBS 2% PFA. Data acquisition was performed on a BD LSR Fortessa Cytometer and data were analysed with FlowJo Software (version 10.7.2).

ICOS measurement in human serums

ICOS protein was quantified by ELISA in the serum of 161 patients with SSc and 38 healthy age- and sex-matched volunteers using the Human ICOS (CD278) ELISA Kit (ThermoFisher Scientific™) according to the manufacturer's instructions.

Statistics

All data analysis were performed using GraphPad Prism 9 Software. Human data were presented as mean with standard deviation (SD) and analyzed with Student's t-test. Mouse data were presented as median with ranges and analyzed by Mann-Whitney Test. Correlation data were analyzed with Spearman's correlation test. A *p* value of less than 0.05 was considered statistically significant.

Results

ICOS expression is increased in serum and skin of SSc patients

We evaluated ICOS expression in the serum of SSc patients (n=161) and healthy controls (n=35). We observed a higher concentration in SSc patients compared to controls: 20.10 ng/mL +/- 31.31 in SSc versus 7.97 ng/mL +/- 6.28 in controls (p=0.024) (Figure 1A). After stratification on skin subsets, we observed no difference between diffuse and limited cutaneous SSc patients: Diffuse 20.91 ng/mL +/-

29.53 (n=68) versus Limited : 19.5ng/mL +/- 32.70 (n=93) (Figure 1B). The sub-group defined by the presence of interstitial lung disease (n=51) was not associated with higher ICOS concentration as compared to patients free of ILD (n=110) (Figure 1B). No other SSc subset including other major organ involvement, disease duration or auto-antibodies, was associated with different serum concentrations.

We next investigated CD3+ ICOS+ T cells in healthy controls and SSc skin taken from dcSSc patients. We observed few and isolated CD3+ ICOS+ T cells in control skin whereas aggregates of CD3+ ICOS+ T cells were readily detected in lesional SSc skin (Figure 1C).

Evaluation of ALPN-101 Efficacy in HOCL-Induced Dermal Fibrosis

ALPN-101 prevents HOCL-induced dermal fibrosis

ALPN-101/HOCL-treated mice had similar body weight changes as observed for the Fc Control/HOCL and PBS group (Figure 2A). As HOCL injections induce skin thickening, we measured dorsal skin folds with a caliper from week 1 to week 6. After 6 weeks of treatment, skin fold thickness was increased by 1.5-fold in HOCL/Fc control-treated mice compared to PBS-treated mice (p=0.0007). ALPN-101 treatment significantly decreased the skin fold thickness by 17.5% compared to HOCL/Fc control-treated mice (p=0.0012) (Figure 2B).

Skin sections from HOCL/Fc control mice were characterized by marked skin thickening as shown in Figure 2C. Dermal thickness was 1.7-fold-increased in HOCL/Fc control-treated mice compared to PBS-treated mice (p=0.0007). A significant decrease of dermal thickness by 25.5% was observed in HOCL/ALPN-101-treated mice compared to HOCL/Fc control treated-mice (p<0.001) (Figure 2C).

Skin collagen content was 1.3-fold higher in HOCL/Fc control mice compared to PBS-treated mice (p=0.003). A significant reduction of collagen content by 20.6% was observed in HOCL/ALPN-101-treated mice compared to HOCL/Fc control-treated mice (Figure 2D).

Fibrillar collagen score as assessed by Second Harmony Generation (SHG) microscopy was 1.3-fold increased in skin sections of HOCL/Fc control-treated mice compared to PBS-treated mice (p=0.34). ALPN-101 treatment decreased fibrillar collagen scores by 38.5% compared to HOCL/Fc control-treated mice (p<0.001) (Figure 2E).

HOCL/Fc control-treated mice had 3.3-fold higher alpha-SMA myofibroblast counts compared to PBS-treated mice (p<0.001). ALPN-101 treatment decreased the number of alpha-SMA positive cells by 47.7% in dermis compared to HOCL/Fc control-treated mice (p=0.016) (Figure 2F).

ALPN-101 reduces immune cell infiltrate in lesional dermis of HOCL mice

T cell (CD3+), B cell (CD20+), macrophage (CD68+), and neutrophil (Ly6G+) numbers were 14.2-, 6.9-, 51- and 33.7-fold higher, respectively, in HOCL/Fc control skin compared to PBS skin (p<0.001) pointing to a striking skin immune infiltration in this model (Figure 3A and B).

ALPN-101 markedly decreased CD68+ macrophages by 40% (p=0.015), Ly6G+ neutrophils by 63.5% (p=0.038), and CD20+ B cells by 34.1% (p=0.049) (Figure 3B). We also observed a trend for ALPN-101-mediated decreases in CD3+ T cells by 37% in the skin of HOCL/ALPN-101-treated mice compared to HOCL/Fc control-treated mice, although this difference did not reach statistical significance (p=0.098) (Figure 3B).

Evaluation of ALPN-101 efficacy in Fra-2 mouse model

ALPN-101 treatment reduces clinical scores in Fra-2 mice

In general, the body weight of mice receiving ALPN-101 was maintained throughout the experiment compared to mice treated with Fc control that lost body weight with age, though the difference between the groups was not statistically significant (Figure 4A, left). Clinical scores evaluating weight loss, coat appearance, and mouse behaviour decreased by 78.4% (p=0.008) and 72.2% (p=0.012), respectively, at the 5^{th} and 6^{th} week in ALPN-101-treated Fra2 Tg mice vs. Fc control-treated Fra2 Tg mice (Figure 4A, right).

ALPN-101 treatment alleviates lung fibrosis and pulmonary hypertension in Fra-2 mice

ALPN-101 treatment decreased collagen content significantly in lungs from Fra-2 Tg mice, by 35.2% (p=0.005) compared to Fc control (Figure 4B). Lung sections of Fc control-treated Fra-2 Tg mice were characterized by large patchy areas of inflammatory infiltrate and collagen deposition (Figure 4C). The histological Ashcroft score of fibrosis was significantly reduced by 33.3% (p= 0.032) in ALPN-101-treated Fra2 Tg mice compared to Fc control-treated Fra2 Tg mice (Figure 4C). SHG microscopy showed an increase of collagen fibers around lung vessels (Figure 4D) in Fc control-treated Fra2 Tg mice. Decreased fibrillar collagen deposition by 47% (p=0.06) was observed in ALPN-101-treated mice compared to Fc control-treated Fra2 Tg mice (Figure 4D).

Regarding pulmonary hypertension (PH), a significant reduction (20.3%, p=0.019) of right ventricular systolic pressure (RVSP) was observed in Fra-2 Tg mice treated with ALPN-101 compared to Fra2 Tg mice that received Fc control treatment.

ALPN-101 reduces T cell response in spleen and lungs of Fra-2 mice

To evaluate the effects of ALPN-101 on T cell responses, we performed flow cytometry analysis by gating on CD4+ and CD8+ populations isolated from the spleen and lungs of treated Fra-2 Tg mice (Supplementary Figure 3). Treatment with ALPN-101 significantly reduced the percentage of CD4+ cells by 11.9% in the spleen (p=0.0381) and by 27.6% in the lungs (p=0.009) compared to Fc control-treated Fra2 Tg mice (Figure 5A). No significant changes in percentages of CD8+ cells were observed between Fc control- and ALPN-101-treated Fra2 Tg mice (Figure 5A). We next investigated the proportions of effector memory T cells (TEM), naïve T cells (T Naïve), and central memory T cells (TCM) based on their differential expression of CD62L and CD44. A significant decrease of CD4+ TEM cells by 43.9 % in spleen

and by 23.8% in lungs (p=0.009) in ALPN-101-treated Fra2 Tg mice was observed compared to Fc control-treated Fra2 Tg mice. The frequency of CD4+ T naive cells was significantly increased by 2.6 times in spleen and by 4 times in lungs (p=0.009) in ALPN-101-treated Fra2-Tg mice compared to Fc control-treated Fra-2 Tg mice (Figure 5B). No differences between Fc control- and ALPN-101-treated Fra2 Tg mice were observed in the proportions of CD4+ TCM, CD8+ TCM, CD8+ TEM, or CD8+ naïve T cells in spleen and lungs.

Activation of CD4+ and CD8+ T cells was assessed based on the expression of the early activation marker CD69 and the T cell exhaustion marker PD-1. The fraction of CD69-expressing cells was significantly reduced by 63.6% within the CD4+ subset in the spleen, (p=0.009) and by 58.2% among CD4+ cells in the lung (p=0.038) upon treatment with ALPN-101 compared to Fc control treatment (Figure 5C). ALPN-101 treatment induced a significant decrease by 60% of CD69-expressing cells among CD8+ spleen cells (p=0.019), but the decrease in CD69-expressing cells within the CD8+ subset in the lung was not statistically significant (p=0.26), compared to Fc control-treated Fra2 Tg mice (Figure 5C). Upon treatment with ALPN-101, a significant 38.2% and 43.2% reduction of PD-1-expressing cells was observed within the CD4+ subset in the spleen (p=0.0095) and in the lung (p=0.038) compared to Fc control treatment, respectively. No changes in the frequency of PD-1-expressing cells were detected within the CD8+ subset in the spleen or lung between the two groups of mice.

Interestingly, we detected a strong correlation between the lung collagen content and CD69 or PD-1 expression in lung CD4+ cells (r=0.9478, p<0.001 and r=0.8545, p=0.003, respectively) (Figure 5D), linking immune activation and extracellular matrix production. Similar findings were observed for CD8+ T cells (Figure 5D).

ALPN-101 serum exposure

We observed 24 hours after ALPN-101 injection similar concentrations between the 10^{th} dose and the 13^{th} dose of ALPN-101 in Fra-2 Tg mice (10^{th} dose, mean ± SD :42630 ± 12112 ng/mL versus 13^{th} dose : 33728 ± 8591 ng/mL) and between the 8^{th} dose and the 13^{th} dose in HOCL-treated mice (8^{th} dose : 24065 ± 13359ng/mL versus 13^{th} dose : 25239 ± 12090ng/mL) (Figure 6A). To track ALPN-101 binding to target cells, we stained cells isolated from spleen and lung with anti-human IgG Fc, which is able to detect the Fc domain of ALPN-101 (Supplementary Figure 4). A significant increase of anti-human IgG staining on spleen and lung CD4+ and CD8+ T cells (p=0.009) was observed in ALPN-101-treated Fra-2 mice compared to Fc control-treated Fra-2 mice (Figure 6B) suggesting ALPN-101 was bound to the majority of T cells. Since ALPN-101 blocks detection of its targets CD28 and ICOS, we first assessed CD28 expression on splenic and lung T cells by flow cytometry, as a method to track target occupancy (Supplementary Figure 4). We observed a reduced detection of CD28 on spleen CD4+ T cells by 99.7% and spleen CD8 T cells by 98.9 % (p=0.009) in ALPN-101-treated Fra2 mice compared to Fc control-treated Fra2 Tg mice. Detection of CD28 was significantly decreased by 66% and by 82.4%, respectively, in lung CD4+ T cells and CD8+ T cells (p=0.0095) isolated from ALPN-101-treated Fra2 Tg mice (Figure 6C). We next analysed ICOS expression on lung and spleen T cells from ALPN-101- and Fc control-treated

Fra-2 Tg mice. Detection of ICOS in spleen cells was significantly decreased by 98.2% on CD4+ (p=0.005) and by 81.2% on CD8+ cells (p=0.009) from ALPN-101-treated Fra2 Tg mice compared to Fc control-treated Fra2 Tg mice. Similar to the spleen results, detection of lung ICOS expression was significantly reduced by 99.7% on CD4+ (p=0.009) and by 88.1% on CD8+ (p=0.009) T cells in ALPN-101-treated Fra2 Tg mice (Figure 6C). These results demonstrated target engagement of ALPN-101 in the spleen and lungs of Fra-2 Tg mice.

Discussion

We herein showed the overexpression of ICOS in SSc patients and demonstrated the efficacy of ALPN-101, a dual CD28/ICOS antagonist, in two complementary mouse models mimicking severe features of SSc patients.

The HOCL-induced dermal fibrosis model, based on induction of oxidative stress by hypochlorite, is characterized by dermal inflammation, fibroblast activation, and collagen production (32) as observed in SSc patients (38). We observed a decrease of dermal thickness, collagen content, myofibroblast number, and inflammatory infiltrate in ALPN-101-treated HOCL-induced mice. These compelling data support a benefit of ALPN-101 treatment in reducing the skin involvement in the HOCL mouse model.

The transgenic Fra-2 mice, in which immune infiltration is followed by pulmonary fibrosis and pulmonary hypertension (33), recapitulates several severe features affecting internal organs of SSc patients (1). Our study demonstrated that ALPN-101 treatment decreased lung fibrosis and collagen content, right ventricular systolic pressure (RVSP), and T cell numbers and activation in Fra-2 Tg mice. The magnitude of the effect of ALPN-101 is in line with other co-stimulation blockade therapies already studied in the Fra-2 model such as abatacept and anti-OX40L antibody (39, 40). Compared to targeted therapies such as the pan-PPAR agonist IVA337, we observed similar levels of lung fibrosis reduction in treated Fra-2 transgenic mice (41). Interestingly, our results showed that CD69 and PD-1 expression on CD4 + T cells was positively correlated with lung collagen content, supporting a link between T cell activation and fibrosis development in the Fra-2 transgenic model. Our results are aligned with previous studies investigating co-stimulation blockade in SSc mouse models. Indeed, a decrease of dermal fibrosis and inflammation after ICOS blockade in GvHD-SSc mice (28) or after intradermal bleomycin injections in $ICOS^{-/-}$ mice compared to WT mice (29) was observed. Other costimulation pathways blockade such as CD28-CD80/CD86 and OX40/OX40-L have previously demonstrated decreased pulmonary and dermal fibrosis in SSc mouse models (39, 40, 42).

In humans, abatacept (CTLA-4-Ig) has been evaluated in a recent phase II study showing a trend of decreased mRSS in early diffuse cutaneous SSc patients treated with abatacept without reaching significance compared to placebo group (11). Interestingly, the decline in mRSS was higher in abatacept-treated patients belonging to inflammatory and normal-like skin gene expression subsets compared to the placebo group, providing support for co-stimulation blockade as a therapeutic strategy for these inflammatory patients.

Our study revealed an increase of ICOS concentration in a large set of SSc patients, extending data obtained in previous studies (26, 27). Moreover, a higher number of circulating T follicular helper cells expressing ICOS was reported in SSc (43) compared to controls; such changes have also been reported in Sjögren's syndrome (44), systemic lupus erythematosus (45), and rheumatoid arthritis (22). These human data were complemented by preclinical work reporting reduced disease progression and humoral responses in lupus nephritis and collagen-induced arthritis mouse models after ICOS-L blockade (46). An anti-ICOSL antibody (AMG557) has been evaluated in patients affected by Sjögren's syndrome (NCT02334306) or by active SLE (NCT04058028) but has revealed no statistically significant efficacy in treated patients compared to placebo group, suggesting that inhibition of the ICOS pathway alone may be insufficient to impact disease. Altogether, the preclinical and clinical results support a role for both the ICOS and CD28 pathways in connective tissue disorders, and our data herein extend the findings to the specific fibrotic phenotype that characterises SSc.

One limitation from the study herein might be that it does not address whether the dual-specific compound ALPN-101 may offer a benefit as compared to single therapies targeting CD28 or ICOS alone, however each single therapy has already demonstrated its relevance in SSc (28, 29, 39, 42) and in other CTDs (46–53). The relevance and added value of the dual antagonist approach has been demonstrated in graft-versus-host disease (GVHD) in which ALPN-101 demonstrated a benefit in a humanized GVHD mouse model by improving survival and preventing T cell activation and expansion as compared to single co-stimulatory pathway inhibitors like CTLA-4-Ig (31). Altogether these and other preclinical data have supported development of acazicolcept (ALPN-101) through a phase 2 program in systemic lupus erythematosus (NCT04835441). Therefore, in order to minimise the number of animals used per experiment, we decided not to include control groups defined by single monoclonal antibodies but to answer to the question of the effects of this bi-specific antibody in the specific context of a fibrotic CTD to evaluate its effects at pre-clinical levels. Notably, a recent clinical study revealed for the first time a significant decrease of the dermatological score mRSS in SSc patients treated with a bi-specific antibody targeting IL-4 and IL-13 (54) ; these findings further support the strategy of targeting multiple pathways in a complex disease like SSc.

Conclusion

We have demonstrated evidence of activation of the ICOS pathway both in serum and skin from SSc patients. Furthermore, our study demonstrated that the concomitant blockade of both ICOS and CD28 pathways with ALPN-101 leads to a significant decrease in dermal and pulmonary fibrosis in two complementary mouse models of SSc. These data supply a piece to the puzzle of inflammation-driven fibrosis and the role of co-stimulatory molecules in the setting of SSc. Our results open the door to follow-up studies where clinical data will be required to establish the translation to patient and to support potential future innovative therapies, especially in the early/inflammatory phase of SSc.

Abbreviations

AF AlexaFluor

alpha-SMA Alpha-smooth Muscular actin

APC Antigen-Presenting Cell

BSA Bovine Serum Albumin

CD Cluster Differentiation

CPP Comité de Protection des Personnes

CTD Connective Tissue Disease

DAB Diaminobenzidine

DAPI 4',6-diamidino-2-phenylindole

dcSSc Diffuse systemic sclerosis

ELISA Enzyme Linked ImmunoSorbent Assay

FBS Fetal Bovine Serum

Fra-2 Fos-related antigen 2

GvHD Graft-versus Host Disease

HES Hematoxylin Eosin Saffron

HLA-DR Human Leucocyte Antigen-DR

HOCL Hypochlorous acid

ICOS Inducible T cell Costimulator

ICOSL Inducible T cell Costimulator Ligand

IHC Immunohistochemistry

IL Interleukin

ILD Interstitial Lung Disease

Ly6G Lymphocyte antigen 6 complex locus GD

mRSS Modified Rodnan Skin Score

PBS Phosphate Buffer saline

PD-1 Programmed Cell Death 1

PFA Paraformaldelhyde

PH Pulmonary hypertension

PPAR Peroxisome proliferator activated receptor

RT Room Temperature

RVSP Right Ventricular Systolic Pressure

SD Standard Deviation

SHG Second Harmony Generation

SPF Specific Pathogen free

SSc Systemic Sclerosis

TCM T central memory

TEM T effector memory

Tfh T follicular Helper

Tg Transgenic

Th T Helper

TPEF Two-photon excited fluorescence

WT Wild-Type

Declarations

Ethical approval and consent to participate

All patients and volunteer blood donors signed a consent form approved by the local institutional review boards [CPP (Comité de Protection des Personnes) Paris Ile de France 3; Convention INSERM, Etablissement français du sang]. Animal protocols used in this study were reviewed and approved by the Ethics committee of our university (Fra-2 protocol : 2019070110126-750V5 ; HOCL protocol : 2019080816497351).

Consent for publication

Not applicable

Availability of supporting data

The datasets used and/or analyzed during the current study are available from the corresponding author on reasonable request. All data generated or analyzed during this study are included in this published article (and its additional information files).

Competing Interests

YA received consulting honorarium from Bayer, Boehringer, Roche, Celltrion, and Sanofi with regards to the management and treatment of systemic sclerosis. NW, MAG, and SRD are employees and shareholders of Alpine Immune Sciences.

Fundings

ALPN-101 drug was supplied by Alpine Immune Sciences. The study was funded by Alpine Immune Sciences. Alpine Immune Sciences was not involved in the study design, data acquisition (except pharmacokinetics), or data analysis.

Authors Contributions

- Study design : YA, JA

- Conduct of experiments : CO, AC, AP, CG, RT, MO, LT, NW, MAG

- Data analysis : CO, AC, AP, FD, CG

- Writing/drafting of the manuscript : CO, AC, SRD, JA, YA

Acknowledgements

We thank platforms from Cochin Institute : photonic imaging platform IMAG'IC (Thomas Guilbert and Pierre Bourdoncle), histology platform HISTIM (Maryline Favier) and cytometry platform CYBIO (Muriel Andrieu). We also thank Drs. Stanford Peng, Jan Hillson, Jing Yang, Katherine Lewis, and Pamela Holland from Alpine Immune Sciences for their input on study design and for their review of the manuscript.

References

1. Allanore Y, Simms R, Distler O, Trojanowska M, Pope J, Denton CP, et al. Systemic sclerosis. Nat Rev Dis Primer déc. 2015;1(1):15002.
2. Elhai M, Meune C, Boubaya M, Avouac J, Hachulla E, Balbir-Gurman A, et al. Mapping and predicting mortality from systemic sclerosis. Ann Rheum Dis nov. 2017;76(11):1897–905.

3. Prescott RJ, Freemont AJ, Jones CJP, Hoyland J, Fielding P. Sequential dermal microvascular and perivascular changes in the development of scleroderma. J Pathol mars. 1992;166(3):255–63.
4. Chizzolini C, Boin F. The role of the acquired immune response in systemic sclerosis. Semin Immunopathol sept. 2015;37(5):519–28.
5. Maehara T, Kaneko N, Perugino CA, Mattoo H, Kers J, Allard-Chamard H, et al. Cytotoxic CD4 + T lymphocytes may induce endothelial cell apoptosis in systemic sclerosis. J Clin Invest 6 avr. 2020;130(5):2451–64.
6. Boleto G, Allanore Y, Avouac J. Targeting Costimulatory Pathways in Systemic Sclerosis. Front Immunol. 18 déc 2018;9:2998.
7. Rudd CE, Schneider H. Unifying concepts in CD28, ICOS and CTLA4 co-receptor signalling. Nat Rev Immunol juill. 2003;3(7):544–56.
8. Esensten JH, Helou YA, Chopra G, Weiss A, Bluestone JA. CD28 Costimulation: From Mechanism to Therapy. Immunity mai. 2016;44(5):973–88.
9. Hutloff A, Dittrich AM, Beier KC, Eljaschewitsch B, Kraft R, Anagnostopoulos I, et al. ICOS is an inducible T-cell co-stimulator structurally and functionally related to CD28. Nature janv. 1999;397(6716):263–6.
10. Gonzalo JA, Tian J, Delaney T, Corcoran J, Rottman JB, Lora J, et al. ICOS is critical for T helper cell–mediated lung mucosal inflammatory responses. Nat Immunol juill. 2001;2(7):597–604.
11. Khanna D, Spino C, Johnson S, Chung L, Whitfield ML, Denton CP, et al. Abatacept in Early Diffuse Cutaneous Systemic Sclerosis: Results of a Phase II Investigator-Initiated, Multicenter, Double-Blind, Randomized, Placebo-Controlled Trial. Arthritis Rheumatol janv. 2020;72(1):125–36.
12. Wikenheiser DJ, Stumhofer JS. ICOS Co-Stimulation: Friend or Foe? Front Immunol [Internet]. 10 août 2016 [cité 9 sept 2021];7. Disponible sur: http://journal.frontiersin.org/Article/10.3389/fimmu.2016.00304/abstract.
13. Garin L, Rigal D, Souillet G, Bernaud J, Mérieux Y, Philippe N. Strong increase in the percentage of the CD8bright + CD28- T-cells and delayed engraftment associated with cyclosporine-induced autologous GVHD. Eur J Haematol 24 avr. 2009;56(3):119–23.
14. Schmidt D, Goronzy JJ, Weyand CM. CD4 + CD7- CD28- T cells are expanded in rheumatoid arthritis and are characterized by autoreactivity. J Clin Invest 1 mai. 1996;97(9):2027–37.
15. Yang J-H, Zhang J, Cai Q, Zhao D-B, Wang J, Guo P-E, et al. Expression and function of inducible costimulator on peripheral blood T cells in patients with systemic lupus erythematosus. Rheumatology 1 oct. 2005;44(10):1245–54.
16. Scarsi M, Ziglioli T, Airo' P. Baseline Numbers of Circulating CD28-negative T Cells May Predict Clinical Response to Abatacept in Patients with Rheumatoid Arthritis. J Rheumatol oct. 2011;38(10):2105–11.
17. Mou D, Espinosa J, Lo DJ, Kirk AD. CD28 Negative T Cells: Is Their Loss Our Gain?: CD28 Negative T Cells. Am J Transplant nov. 2014;14(11):2460–6.

18. Żabińska M, Krajewska M, Kościelska-Kasprzak K, Klinger M. CD3 $^{+}$ CD8 $^{+}$ CD28 $^{-}$ T Lymphocytes in Patients with Lupus Nephritis. J Immunol Res. 2016;2016:1–7.
19. Piantoni S, Regola F, Zanola A, Andreoli L, Dall'Ara F, Tincani A, et al. Effector T-cells are expanded in systemic lupus erythematosus patients with high disease activity and damage indexes. Lupus janv. 2018;27(1):143–9.
20. Sato T, Kanai T, Watanabe M, Sakuraba A, Okamoto S, Nakai T, et al. Hyperexpression of inducible costimulator and its contribution on lamina propria T cells in inflammatory bowel disease. Gastroenterology mars. 2004;126(3):829–39.
21. Christensen JR, Börnsen L, Ratzer R, Piehl F, Khademi M, Olsson T, et al. Systemic Inflammation in Progressive Multiple Sclerosis Involves Follicular T-Helper, Th17- and Activated B-Cells and Correlates with Progression. Filion LG, éditeur. PLoS ONE 1 mars. 2013;8(3):e57820.
22. Wang J, Shan Y, Jiang Z, Feng J, Li C, Ma L, et al. High frequencies of activated B cells and follicular helper T cells are correlated with disease activity in patients with new onset rheumatoid arthritis: High frequency of TFH and B cells in RA patients. Clin Exp Immunol. juin 2013;n/a-n/a.
23. Choi J-Y, Ho JH, Pasoto SG, Bunin V, Kim ST, Carrasco S, et al. Circulating Follicular Helper-Like T Cells in Systemic Lupus Erythematosus: Association With Disease Activity: Circulating Tfh-Like Cells in SLE. Arthritis Rheumatol avr. 2015;67(4):988–99.
24. Fonseca VR, Romão VC, Agua-Doce A, Santos M, López-Presa D, Ferreira AC, et al. The Ratio of Blood T Follicular Regulatory Cells to T Follicular Helper Cells Marks Ectopic Lymphoid Structure Formation While Activated Follicular Helper T Cells Indicate Disease Activity in Primary Sjögren's Syndrome. Arthritis Rheumatol mai. 2018;70(5):774–84.
25. Cheng LE, Amoura Z, Cheah B, Hiepe F, Sullivan BA, Zhou L, et al. Brief Report: A Randomized, Double-Blind, Parallel-Group, Placebo-Controlled, Multiple-Dose Study to Evaluate AMG 557 in Patients With Systemic Lupus Erythematosus and Active Lupus Arthritis. Arthritis Rheumatol juill. 2018;70(7):1071–6.
26. Yanaba K, Asano Y, Noda S, Akamata K, Aozasa N, Taniguchi T, et al. Increased production of soluble inducible costimulator in patients with diffuse cutaneous systemic sclerosis. Arch Dermatol Res janv. 2013;305(1):17–23.
27. Hasegawa M, Fujimoto M, Matsushita T, Hamaguchi Y, Takehara K. Augmented ICOS expression in patients with early diffuse cutaneous systemic sclerosis. Rheumatol Oxf Engl févr. 2013;52(2):242–51.
28. Taylor DK, Mittereder N, Kuta E, Delaney T, Burwell T, Dacosta K, et al. T follicular helper–like cells contribute to skin fibrosis. Sci Transl Med. 7 mars 2018;10(431):eaaf5307.
29. Tanaka C, Fujimoto M, Hamaguchi Y, Sato S, Takehara K, Hasegawa M. Inducible costimulator ligand regulates bleomycin-induced lung and skin fibrosis in a mouse model independently of the inducible costimulator/inducible costimulator ligand pathway. Arthritis Rheum 26 févr. 2010;62(6):1723–32.
30. Goenka R, Xu Z, Samayoa J, Banach D, Beam C, Bose S, et al. CTLA4-Ig–Based Bifunctional Costimulation Inhibitor Blocks CD28 and ICOS Signaling to Prevent T Cell Priming and Effector

Function. J Immunol 1 mars. 2021;206(5):1102–13.

31. Adom D, Dillon SR, Yang J, Liu H, Ramadan A, Kushekhar K, et al. ICOSL $^{+}$ plasmacytoid dendritic cells as inducer of graft-versus-host disease, responsive to a dual ICOS/CD28 antagonist. Sci Transl Med. oct 2020;7(564):eaay4799. 12(.
32. Servettaz A, Goulvestre C, Kavian N, Nicco C, Guilpain P, Chéreau C, et al. Selective Oxidation of DNA Topoisomerase 1 Induces Systemic Sclerosis in the Mouse. J Immunol 1 mai. 2009;182(9):5855–64.
33. Birnhuber A, Biasin V, Schnoegl D, Marsh LM, Kwapiszewska G. Transcription factor Fra-2 and its emerging role in matrix deposition, proliferation and inflammation in chronic lung diseases. Cell Signal déc. 2019;64:109408.
34. Eferl R, Hasselblatt P, Rath M, Popper H, Zenz R, Komnenovic V, et al. Development of pulmonary fibrosis through a pathway involving the transcription factor Fra-2/AP-1. Proc Natl Acad Sci 29 juill. 2008;105(30):10525–30.
35. Maurer B, Reich N, Juengel A, Kriegsmann J, Gay RE, Schett G, et al. Fra-2 transgenic mice as a novel model of pulmonary hypertension associated with systemic sclerosis. Ann Rheum Dis août. 2012;71(8):1382–7.
36. Ashcroft T, Simpson JM, Timbrell V. Simple method of estimating severity of pulmonary fibrosis on a numerical scale. J Clin Pathol 1 avr. 1988;41(4):467–70.
37. Gailhouste L, Grand YL, Odin C, Guyader D, Turlin B, Ezan F, et al. Fibrillar collagen scoring by second harmonic microscopy: A new tool in the assessment of liver fibrosis. J Hepatol mars. 2010;52(3):398–406.
38. Gabrielli A. New Insights into the Role of Oxidative Stress in Scleroderma Fibrosis. Open Rheumatol J 15 juin. 2012;6(1):87–95.
39. Boleto G, Guignabert C, Pezet S, Cauvet A, Sadoine J, Tu L, et al. T-cell costimulation blockade is effective in experimental digestive and lung tissue fibrosis. Arthritis Res Ther déc. 2018;20(1):197.
40. Elhai M, Avouac J, Hoffmann-Vold AM, Ruzehaji N, Amiar O, Ruiz B, et al. OX40L blockade protects against inflammation-driven fibrosis. Proc Natl Acad Sci 5 juill. 2016;113(27):E3901–10.
41. Avouac J, Konstantinova I, Guignabert C, Pezet S, Sadoine J, Guilbert T, et al. Pan-PPAR agonist IVA337 is effective in experimental lung fibrosis and pulmonary hypertension. Ann Rheum Dis nov. 2017;76(11):1931–40.
42. Ponsoye M, Frantz C, Ruzehaji N, Nicco C, Elhai M, Ruiz B, et al. Treatment with abatacept prevents experimental dermal fibrosis and induces regression of established inflammation-driven fibrosis. Ann Rheum Dis déc. 2016;75(12):2142–9.
43. Ricard L, Jachiet V, Malard F, Ye Y, Stocker N, Rivière S, et al. Circulating follicular helper T cells are increased in systemic sclerosis and promote plasmablast differentiation through the IL-21 pathway which can be inhibited by ruxolitinib. Ann Rheum Dis avr. 2019;78(4):539–50.
44. Szabo K, Papp G, Barath S, Gyimesi E, Szanto A, Zeher M. Follicular helper T cells may play an important role in the severity of primary Sjögren's syndrome. Clin Immunol mai. 2013;147(2):95–104.

45. Simpson N, Gatenby PA, Wilson A, Malik S, Fulcher DA, Tangye SG, et al. Expansion of circulating T cells resembling follicular helper T cells is a fixed phenotype that identifies a subset of severe systemic lupus erythematosus. Arthritis Rheum janv. 2010;62(1):234–44.
46. Hu Y-L, Metz DP, Chung J, Siu G, Zhang M. B7RP-1 Blockade Ameliorates Autoimmunity through Regulation of Follicular Helper T Cells. J Immunol 1 févr. 2009;182(3):1421–8.
47. Pontarini E, Murray-Brown WJ, Croia C, Lucchesi D, Conway J, Rivellese F, et al. Unique expansion of IL-21 + Tfh and Tph cells under control of ICOS identifies Sjögren's syndrome with ectopic germinal centres and MALT lymphoma. Ann Rheum Dis déc. 2020;79(12):1588–99.
48. Frey O, Meisel J, Hutloff A, Bonhagen K, Bruns L, Kroczek RA, et al. Inducible costimulator (ICOS) blockade inhibits accumulation of polyfunctional T helper 1/T helper 17 cells and mitigates autoimmune arthritis. Ann Rheum Dis 1 août. 2010;69(8):1495–501.
49. Iwai H, Abe M, Hirose S, Tsushima F, Tezuka K, Akiba H, et al. Involvement of Inducible Costimulator-B7 Homologous Protein Costimulatory Pathway in Murine Lupus Nephritis. J Immunol 15 sept. 2003;171(6):2848–54.
50. Laurent L, Le Fur A, Le Bloas R, Néel M, Mary C, Moreau A, et al. Prevention of lupus nephritis development in NZB/NZW mice by selective blockade of CD28. Eur J Immunol août. 2017;47(8):1368–76.
51. Vierboom MPM, Breedveld E, Kap YS, Mary C, Poirier N, 't Hart BA, et al. Clinical efficacy of a new CD28-targeting antagonist of T cell co-stimulation in a non-human primate model of collagen-induced arthritis: Targeting CIA with CD28 antagonist. Clin Exp Immunol mars. 2016;183(3):405–18.
52. Shi Q, Gao ZY, Xie F, Wang LF, Gu YP, Yang TJ, et al. A Novel Monoclonal Antibody against Human CD80 and its Immune Protection in a Mouse Lupus-like Disease. Int J Immunopathol Pharmacol juill. 2011;24(3):583–93.
53. Webb LMC, Walmsley MJ, Feldmann M. Prevention and amelioration of collagen-induced arthritis by blockade of the CD28 co-stimulatory pathway: requirement for both B7-1 and B7-2. Eur J Immunol oct. 1996;26(10):2320–8.
54. Allanore Y, Wung P, Soubrane C, Esperet C, Marrache F, Bejuit R, et al. A randomised, double-blind, placebo-controlled, 24-week, phase II, proof-of-concept study of romilkimab (SAR156597) in early diffuse cutaneous systemic sclerosis. Ann Rheum Dis déc. 2020;79(12):1600–7.

Figures

Figure 1

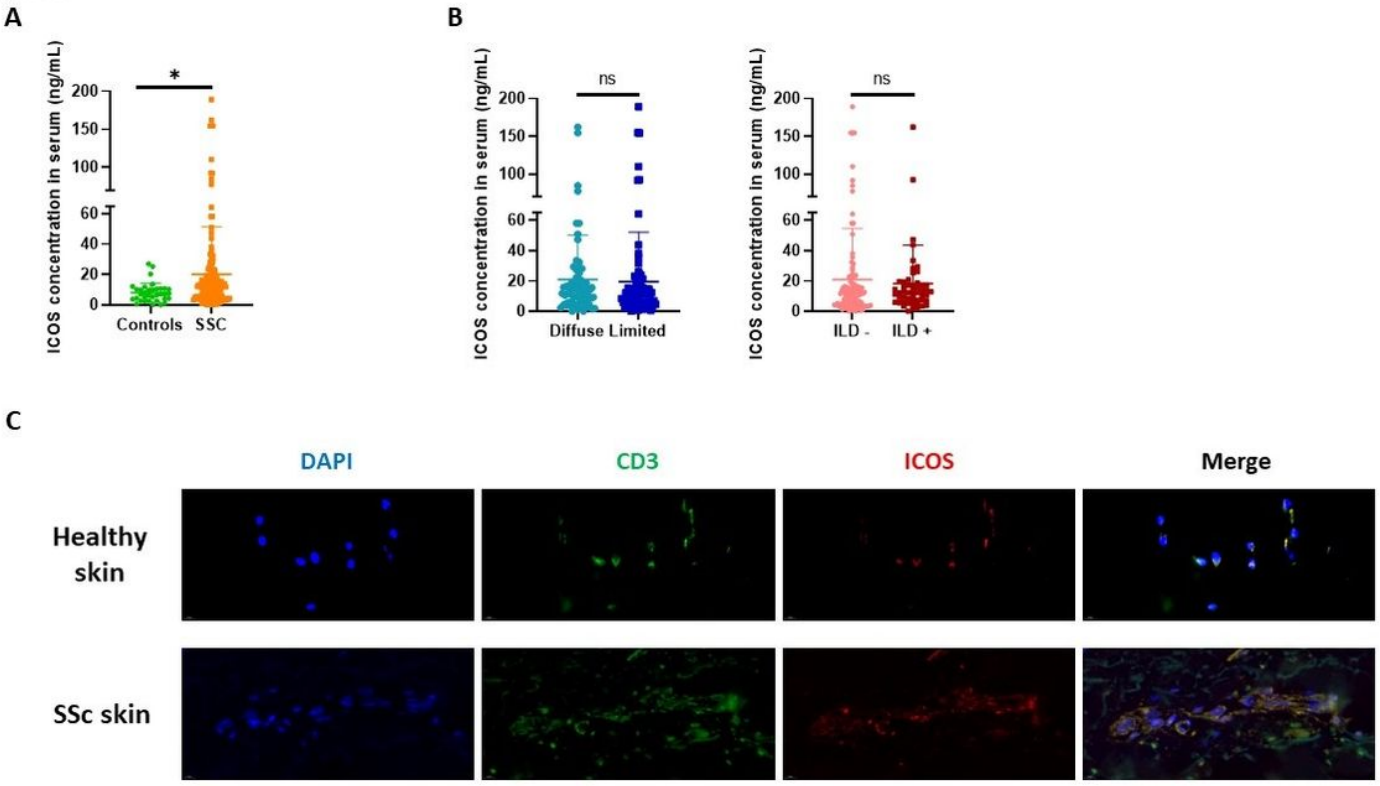

Figure 1

ICOS is increased in SSc serum. (A) ICOS concentration in serum from healthy controls (n=35) and SSc patients (n=161). (B) ICOS concentration in serum of SSc patients divided for diffuse/limited disease or interstitial lung disease or not. (C) Representative images of CD3+ and ICOS+ staining in dermal skin from healthy controls and SSc patients (magnification x100). Horizontal lines represent the mean and error bars depict the standard deviation. *p<0.05 by Student's t-test. ns = not significant.

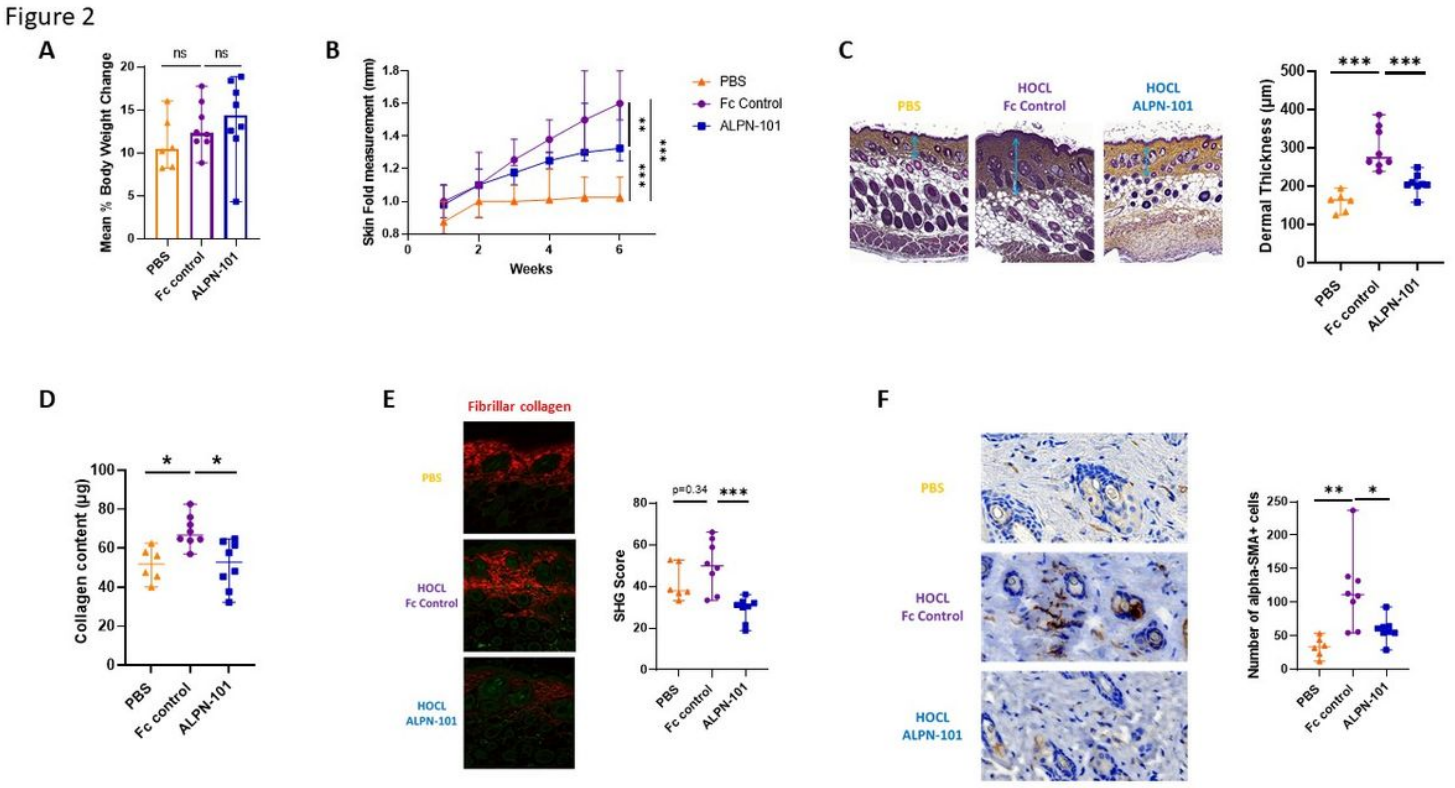

Figure 2

ALPN-101 alleviates dermal fibrosis development in the HOCL mouse model. (A) Mean percentage of body weight change calculated between first week and sixth week of treatment (B) Measurements of skin fold thickness in millimeters from week 1 to week 6, collected weekly. (C) Left : Representative HES 4 µm-skin sections of PBS/, HOCL/Fc control- and HOCL/ALPN-101-treated mice (Objectif x15). Arrows represents the dermal thickness measurement on each skin section. Right : Mean of five measurements of dermal thickness for each mouse in micrometers. (D) Content of collagen in a 3-mm dorsal skin punch evaluated by Sircol assay in PBS-, HOCL/Fc control- and HOCL/ALPN-101-treated mice. (E) Left : Representative SHG images of 16 µm dorsal skin sections from PBS/, HOCL/Fc control- and HOCL/ALPN-101-treated mice. Right : Scoring of fibrillar collagen in PBS/, HOCL/Fc control- and HOCL/ALPN-101-treated dorsal skin sections. (F) Left : Representative IHC staining of alpha-SMA (brown) in 4 µm skin sections counterstained with hematoxylin of PBS/, HOCL/Fc control- and HOCL/ALPN-101-treated mice (magnification x100). Right : Number of alpha-SMA positive cells in a 4 µm-dorsal skin section from PBS/, HOCL/Fc control- and HOCL/ALPN-101-treated mice. Mice were divided into three groups : PBS/treated group (n=6), HOCL/Fc control-treated group (n=8) and HOCL/ALPN-101-treated group (n=8). Horizontal lines represent the median with range. *p<0.05 ; **p<0.01 ; ***p<0.001 by Mann-Whitney U test.

Figure 3

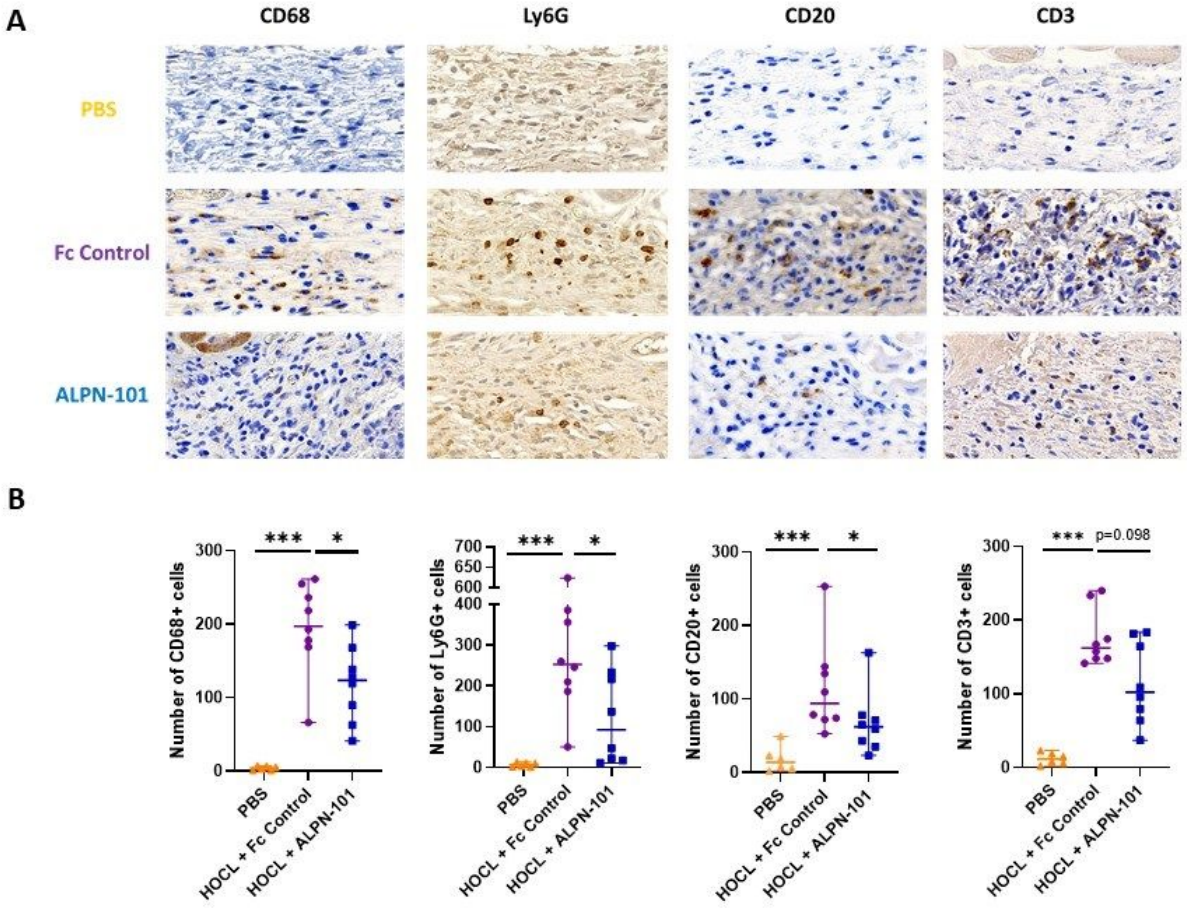

Figure 3

ALPN-101 decreased immune cell infiltrates in lesional skin of HOCL-treated mice. (A) Representative IHC staining (brown) of macrophages (CD68+), neutrophils (Ly6G+), B cells (CD20+) and T cells (CD3+) on 4 µm dorsal skin sections counterstained with hematoxylin from PBS/, HOCL/Fc control- and HOCL/ALPN-101-treated mice (magnification x120). (B) Number of CD68, Ly6G, CD20, or CD3-positive cells in a 4 µm-dorsal skin section from PBS/, HOCL/Fc control- and HOCL/ALPN-101-treated mice. Mice were divided into three groups : PBS group (n=6), HOCL/Fc control-treated group (n=8) and HOCL/ALPN-101-treated groups (n=8). Horizontal lines represent the median with range. *p<0.05 ; **p<0.01 ; ***p<0.001 by Mann-Whitney U test. ns= not significant.

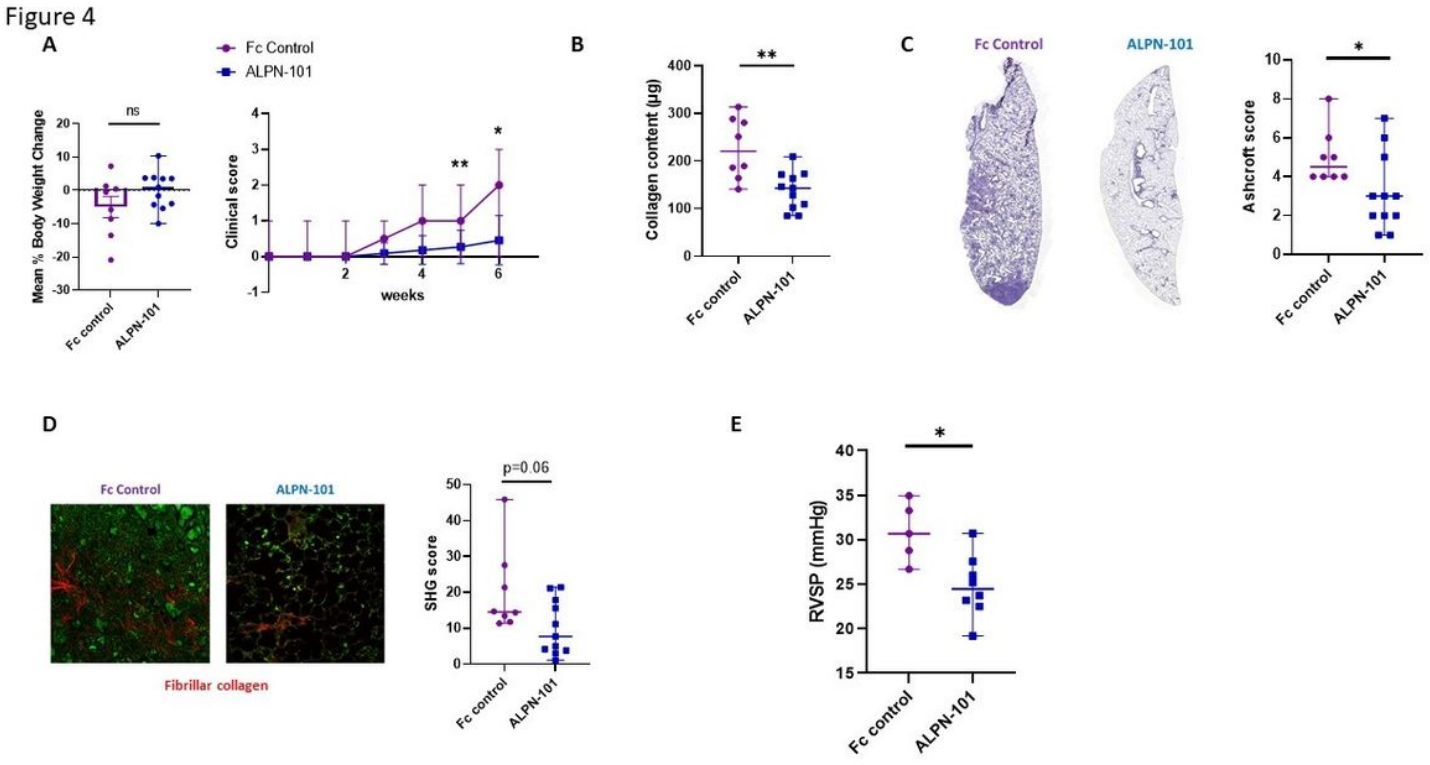

Figure 4

ALPN-101 protects against development of lung fibrosis in Fra-2 mice model. (A) Left : Mean percentage of body weight change calculated between first week and sixth week of treatment. Right : Clinical score follow-up during the six weeks of treatment based on body weight, coat appearance, and mouse behaviour. (B) Content of collagen in a lung fragment (µg) evaluated by Sircol assay in Fc control- and ALPN-101-treated Fra-2 Tg mice. (C) Left : Representative HES 4 µm lung sections of Fc control- and ALPN-101-treated mice. Right : Ashcroft histological score of Fc control- and ALPN-101-treated Fra-2 Tg mice. (D) Left : Representative SHG images of 16 µm lung sections from Fc control- and ALPN-101-treated Fra-2 Tg mice (magnification x25). Collagen fibers are coloured in red. Right : Scoring of fibrillar collagen in lung sections from Fc control and ALPN-101-treated mice. (E) Measure of right ventricular systolic pressure (mmHg) of Fc control- and ALPN-101-treated Fra-2 Tg mice after right catheterization of mice. Fra-2 mice were divided into two groups : Fc control-treated (n=8) and ALPN-101-treated (n=11). Horizontal lines represent the median with range. *p<0.05 ; **p<0.01 ; by Mann-Whitney U test. ns= no significant.

Figure 5

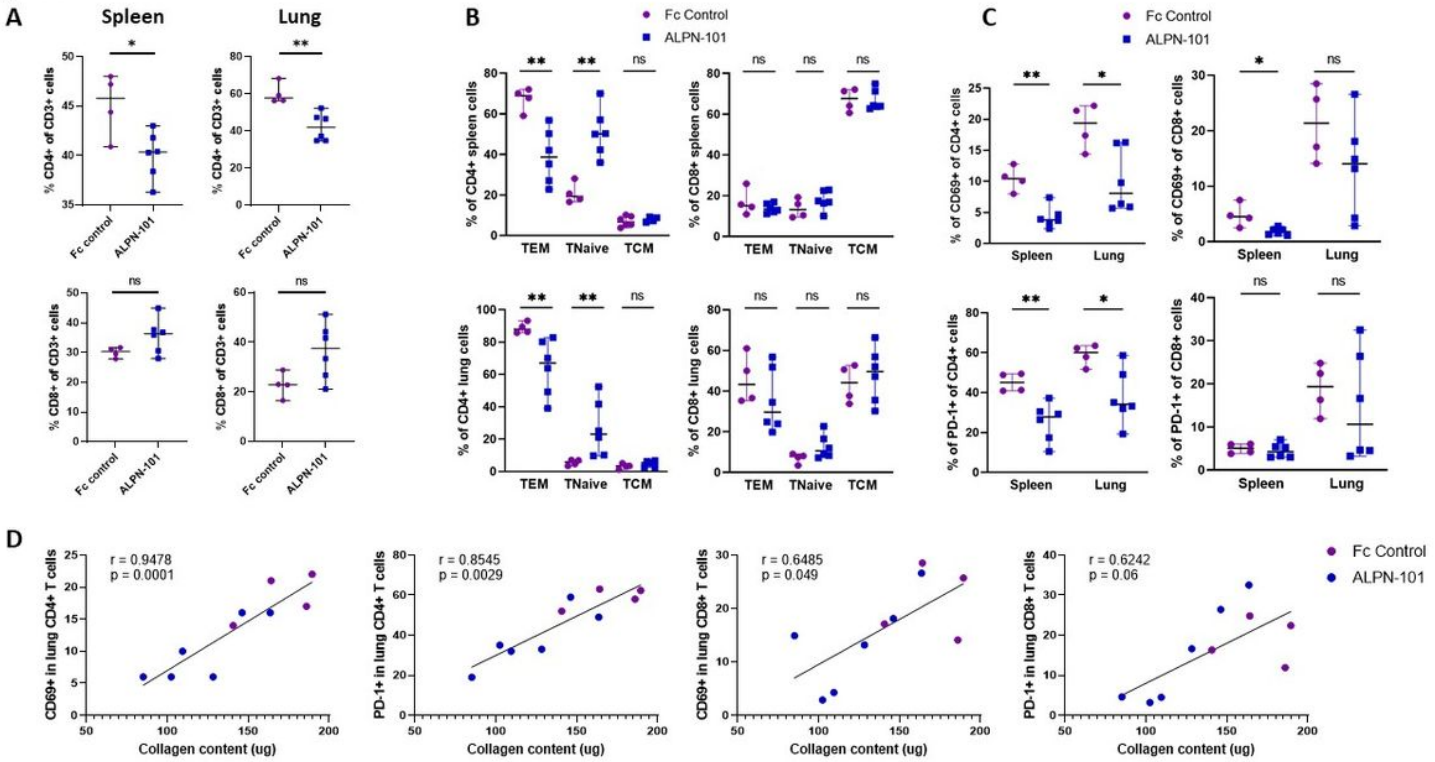

Figure 5

ALPN-101 decreased T cell activation in lungs and spleen of Fra-2 mice. (A) Percentages of CD4+ and CD8+ T cells in CD3+ T cells of the spleen and the lung of Fc control- and ALPN-101-treated mice. (B) Percentage of CD4+ or CD8+ effector memory T cells (TEM : CD62L- CD44+), naïve T (CD62L+ CD44-) and central memory T cells (TCM : CD62L+ CD44+) in spleen and lungs of Fc control- and ALPN-101-treated Fra-2 Tg mice. (C) Percentage of CD69- and PD-1-positive cells within CD4+ or CD8+ subsets in spleen and lungs of Fc control- and ALPN-101-treated Fra-2 Tg mice. (D) Spearman correlation between CD69 and PD-1 expression on lung CD4/CD8 T cells evaluated by flow cytometry and lung collagen content evaluated by Sircol assay. Flow cytometry analysis was performed on 4 spleen/lungs from Fc control-treated mice and on 6 spleen/lungs of ALPN-101-treated Fra-2 Tg mice. Horizontal lines represent the median with range *p<0.05 ; **p<0.01 ; ***p<0.001 by Mann-Whitney U test. ns= not significant.

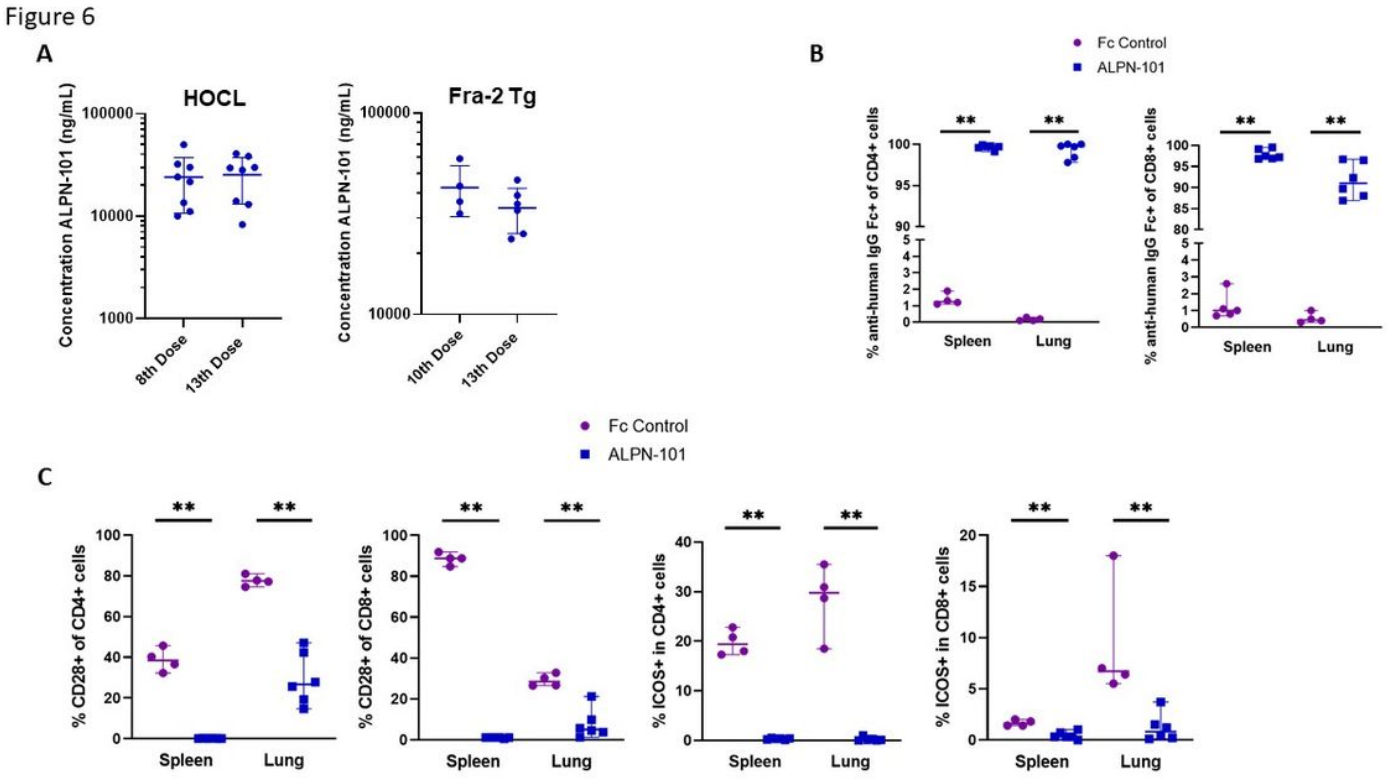

Figure 6

ALPN-101 serum exposure. (A) Left : Measurement of ALPN-101 concentrations in HOCL-treated mouse serum 24 hours after the 8th (n=8) or the 13th dose (n=8). Right : Measurement of ALPN-101 concentrations in Fra-2 Tg mouse serum collected 24 hours after the 10th (n=4) or the 13th dose (n=6). Right : (B) Percentage of anti-human IgG Fc-binding cells among CD4+ or CD8+ cells from spleen and lungs of Fc control (n=4)- or ALPN-101 (n=6)-treated mice as measured by flow cytometry. (C) Percentage of ICOS- and CD28-positive cells in CD4+ or CD8+ T cells from the lungs and spleen of Fc control (n=4)- and ALPN-101 (n=6)-treated mice as measured by flow cytometry. Horizontal lines represent the median with range *p<0.05 ; **p<0.01 ; by Mann-Whitney U test.

Supplementary Files

This is a list of supplementary files associated with this preprint. Click to download.

- SupplementaryFigure1.pptx
- SupplementaryFigure2.pptx
- SupplementaryFigure3.pptx
- SupplementaryFigure4.pptx